Acta Crystallographica Section D
Biological Crystallography
ISSN 0907-4449

Structure of human transthyretin complexed with bromophenols: a new mode of binding

Minakshi Ghosh,[a]* Ilonka A. T. M. Meerts,[b] Atlanta Cook,[a] Ake Bergman,[c] Abraham Brouwer[b,d] and Louise N. Johnson[a]

[a]Laboratory of Molecular Biophysics, Department of Biochemistry, South Parks Road, Oxford OX1 3QU, England, [b]Toxicology Group, Department of Food Technology and Nutritional Sciences, Wageningen University and Research Centre, Tuinlaan 5, PO Box 6700 EA Wageningen, The Netherlands, [c]Department of Environmental Chemistry, Stockholm University, SE-106 91 Stockholm, Sweden, and [d]Institute of Environmental Studies, Free University of Amsterdam, 1081 HV Amsterdam, The Netherlands

Correspondence e-mail: mina@biop.ox.ac.uk

Received 4 February 2000
Accepted 16 June 2000

PDB References: TTR, 1e3f; TTR–PBP, 1e4h; TTR–TBP, 1e5a.

The binding of two organohalogen substances, pentabromophenol (PBP) and 2,4,6-tribromophenol (TBP), to human transthyretin (TTR), a thyroid hormone transport protein, has been studied by *in vitro* competitive binding assays and by X-ray crystallography. Both compounds bind to TTR with high affinity, in competition with the natural ligand thyroxine (T_4). The crystal structures of the TTR–PBP and TTR–TBP complexes show some unusual binding patterns for the ligands. They bind *exclusively* in the 'reversed' mode, with their hydroxyl group pointing towards the mouth of the binding channel and in planes approximately perpendicular to that adopted by the T_4 phenolic ring in a TTR–T_4 complex, a feature not observed before. The hydroxyl group in the ligands, which was previously thought to be a key ingredient for a strong binding to TTR, does not seem to play an important role in the binding of these compounds to TTR. In the TTR–PBP complex, it is primarily the halogens which interact with the TTR molecule and therefore must account for the strong affinity of binding. The interactions with the halogens are smaller in number in TTR–TBP and there is a decrease in affinity, even though the interaction with the hydroxyl group is stronger than that in the TTR–PBP complex.

1. Introduction

Organohalogen substances (OHSs) are present as residues in the environment for several reasons. They are generated either as by-products formed in the commercial production of industrial chemicals or by further reactions of the chemicals during combustion processes. They can also be the result of metabolic processes if these chemicals are absorbed by living organisms. These compounds have a wide range of application as pesticides, adhesives, flame retardants, dielectric fluid for transformers and capacitors, lubricants, sealants and even in carbonless copy paper (Safe, 1994). In recent years, it has been shown that exposure to these compounds can adversely affect the thyroid hormone system in animals and humans (Brouwer *et al.*, 1998). One level of interference of OHSs with the thyroid hormone system is through interactions with transthyretin (TTR), one of the proteins responsible for the transport of the thyroid hormones in blood plasma. A relatively constant level of free thyroid hormones in the blood is maintained by equilibrium reactions with the transport proteins to which more than 99% of the hormones are bound (Robbins, 1991). Any variation in the hormone binding with the transport proteins can therefore affect the level of free hormones in the blood. Severe reductions in thyroxine levels in the plasma of laboratory animals, wildlife and humans have

been reported following exposures to OHSs such as polychlorinated biphenyls (PCBs) and polybrominated biphenyls (PBBs) (Brouwer *et al.*, 1998; Pluim *et al.*, 1993; Van den Berg *et al.*, 1988). *In vitro* binding studies with several groups of OHSs have shown that these compounds are able to bind to TTR with a potency comparable to or higher than that of the natural ligand thyroxine (T_4) (Lans *et al.*, 1993, 1994). In contrast, these compounds do not bind with thyroxine-binding globulin (TBG), the major carrier of thyroid hormones in mammals (Lans *et al.*, 1993; Rickenbacher *et al.*, 1986; Van den Berg, 1990; Van Raaij *et al.*, 1991). The depletion of the thyroxine levels in blood of the laboratory animals following exposure to OHSs may therefore be explained by competitive binding of these organohalogens to TTR, inhibiting the interaction of the protein with its natural ligand T_4 or other iodothyronines.

In vitro binding studies have shown that the OHSs bind to TTR with a wide-ranging affinity for the protein and attempts have been made to find a correlation between the structure and affinity of the ligands. The degree of halogen substitution was found to be important, as the higher halogenated phenols (Van den Berg, 1990) and bisphenols (Meerts *et al.*, 2000) showed a higher affinity for the T_4 binding site compared with the lower halogenated compounds. The presence of a hydroxyl group at the *para* or *meta* positions of the phenyl rings of polychlorinated biphenyls, with at least one chlorine substitution at an adjacent position, was thought to be an essential prerequisite for TTR binding (Lans *et al.*, 1993). However, it has also been shown that some parent compounds without the hydroxyl group are capable of binding TTR (Chauhan *et al.*, 1998; Meerts, unpublished results), though the binding is weak.

In order to obtain a better understanding about the nature of the interaction of OHSs with TTR at the molecular level, we studied two brominated compounds (Fig. 1), pentabromophenol (PBP) and 2,4,6-tribromophenol (TBP). Here, we present the results of *in vitro* TTR–T_4 competitive binding experiments with these compounds using radiolabelled thyroxine ^{125}I-T_4 and the structural details of ligand binding as determined by X-ray crystallography at 100 K.

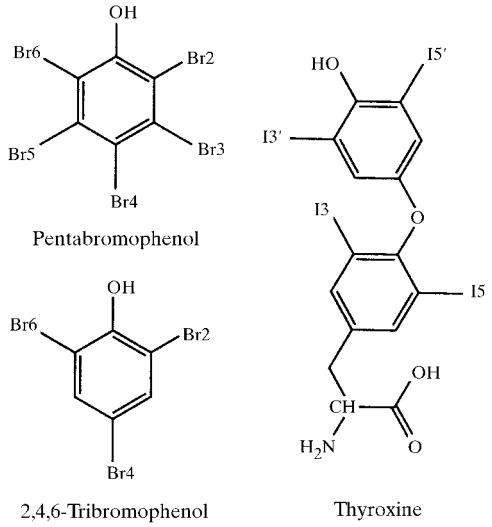

Figure 1
Schematic diagram of pentabromophenol, 2,4,6-tribromophenol and thyroxine.

2. Experimental procedures

2.1. Binding studies

2.1.1. *In vitro* T_4 competition binding assays on TTR. A competition binding assay using the gel-filtration procedure (Somack *et al.*, 1982) was used with minor modifications to measure the ability of the PBP (Aldrich Chemical Company, Bornem, Belgium) and TBP (Fluka Chemie, Buchs, Switzerland) to displace radiolabelled L-3′,5′-(^{125}I) thyroxine from the high-affinity TTR-binding site. The assay buffer used was 0.1 *M* Tris–HCl pH 8.0 containing 0.1 *M* NaCl and 1 m*M* EDTA. The incubation mixture contained 30 n*M* human TTR (98% pure, Sigma, USA), a mixture (70 000 counts min^{-1}, 55 n*M*) of ^{125}I-T_4 (specific activity 46 µCi µg^{-1}, Amersham, UK) and unlabelled T_4 (Sigma, USA) and graded concentrations of competitor (unlabeled T_4 or PBP/TBP dissolved in dimethylsulfoxide, 99.9% pure, Janssen Chimica, Geel, Belgium) in assay buffer. The final concentration of the unlabelled compounds was in the range 10^{-9} to 10^{-7} *M*. The final volume of the incubation mixture was 0.2 ml. The total ^{125}I radioactivity added to each of the incubation mixtures was checked by gamma-counting (Multi Prias, Packard Instrument Co., USA). The incubation mixtures were allowed to reach binding equilibrium overnight at 277 K. Biogel P-6DG (Bio-Rad Laboratories, Richmond, CA, USA) columns were prepared in a 1 ml disposable syringe, equilibrated with the assay incubation buffer and 300 µl 10%(*w*/*v*) sucrose/Tris–HCl buffer. Protein-bound ^{125}I-T_4 and free ^{125}I-T_4 were spin-forced separated on the columns by centrifugation at 1000 rev min^{-1} (100*g*) in a precooled centrifuge (Difuge, Hereaus). The columns were spin-forced eluted with an additional volume of 200 µl Tris–HCl buffer. Radioactivity in the eluate fraction was determined and compared with control incubations.

2.1.2. Analysis of binding data. Competition binding curves were made by plotting relative ^{125}I-T_4 protein binding (percentage of control) against added log competitor concentration. Calculation of binding parameters was performed with the *LIGAND-PC* program (Munson & Rodbard, 1980). Each assay contained duplicate measurements and assays were repeated three times. The binding potency of PBP/TBP relative to that of thyroxine was calculated by the ratio of unlabelled T_4 concentration at 50% of total binding $IC_{50}(T_4)$ to ligand concentration at 50% of total binding (IC_{50} PBP/TBP). Competition binding assays with unlabelled T_4 were used as reference assays.

2.2. X-ray crystallographic studies

2.2.1. Co-crystallization of the TTR–bromophenol complexes. Solutions of PBP (6.1 m*M*) and TBP (14.6 m*M*) were prepared by dissolving the compounds in DMSO (Sigma,

UK). To form the complexes, 25 µl of TTR (Sigma, UK) solution (0.37 m*M* in 100 m*M* Tris buffer containing 100 m*M* NaCl and 1 m*M* EDTA at pH 8) was mixed with 2 µl of each of the bromophenol solutions in microbridges which were then sealed with cover slips and allowed to incubate for 1 d at 277 K. The final molar concentrations were in the ratio 34:45 and 34:110 for TTR:PBP and TTR:TBP, respectively. Two sets of crystallizations were set up at 295 and 277 K, respectively, in 2 µl hanging drops containing protein–ligand complex and the precipitants in 1:1(*v*/*v*) ratio and were allowed to equilibrate over a reservoir of 50–55% ammonium sulfate in 100 m*M* sodium citrate buffer pH 7. Crystals appeared in the drops at 295 K after nearly two months. Native TTR crystals were grown under similar conditions.

2.2.2. Data collection. Cryogenic techniques (Garman & Schneider, 1997) were used for collecting the diffraction data. A complete set of data was collected from a single frozen crystal in each case, using a 30 cm MAR Research image-plate detector mounted on a Rigaku RU-200 rotating-anode source of Cu $K\alpha$ X-radiation. Prior to freezing, 10 µl drops of glycerol solution in the crystallization buffer were gradually added to the drops containing the crystals so that the concentration of glycerol in the drop increased approximately to 40% to prevent ice formation in the crystal at sub-zero temperatures. The crystals were then transferred by means of tiny woollen loops and flash-frozen in a stream of cold gaseous nitrogen at 100 K and were kept at that temperature during the entire data collection. The crystal-to-detector distance was set at 120 mm for the complex crystals, the resolution at the edge of the detector being 1.8 Å; for the native crystal, the detector distance was 116 mm (1.75 Å at the edge). The data were processed using the programs *DENZO* and *SCALEPACK* (Otwinowski & Minor, 1997). For the native crystal, the reflections beyond 1.9 Å were not used because of poor $I/\sigma(I)$ and $R_{\rm merge}$ values. Structure factors were derived from intensities using the program *TRUNCATE* from the *CCP*4 package (Collaborative Computational Project, Number 4, 1994). All three types of crystals were isomorphous to native TTR crystals at room temperature (Blake *et al.*, 1978; Hamilton *et al.*, 1992) and belonged to the orthorhombic space group $P2_12_12$.

2.2.3. Refinement and validation of the final structure. Refinement of the structures was carried out by alternate cycles of the *X-PLOR* package version 3.851 (Brünger, 1992) and manual fitting of the model into the electron-density maps using *O* (Jones & Kjeldgaard, 1997). The structure of native transthyretin, solved at room temperature to 1.7 Å resolution (Hamilton *et al.*, 1992), was used as a starting model; the N-terminal residues (1–9) and C-terminal residues (124–127) were removed as these were not well ordered in the native structure. Residues with double conformations were initially replaced by alanines. 5% of the reflections were set aside for use as a test set to monitor the refinement process by calculating $R_{\rm free}$ (Brünger, 1992). Initially, the two monomers in the asymmetric unit were refined as two rigid objects. Fourier and difference Fourier maps calculated at this stage clearly showed the positions of the ligands in the binding channel, the peaks corresponding to the halogen atoms being the highest in the maps.

The coordinates of the pentabromophenol (PBP) molecule were obtained from the Cambridge Structural Database using *QUEST* (Allen & Kennard, 1993). The molecule was fitted into the electron-density map and included in the model for structure-factor calculations in the subsequent refinements. PBP was found to bind at two ligand-binding sites symmetrically on the crystallographic dyad along *z*, which runs along the binding channel. At each site, one half of the molecule was included in the atomic coordinate set with occupancy 1, while the other half was generated by the twofold rotation about *z*. At one of these binding sites there was evidence of an additional low-occupancy binding for the PBP molecule. Only the Br atoms of the molecule could be detected on the $2F_o - F_c$ map, where no density was to be seen for the C atoms on the ring structure of the molecule. However, the observed five peaks fitted exactly with the Br-atom positions in PBP. This defined the position of the ligand in this mode without any ambiguity. The peak heights for these Br atoms were comparable to those of O atoms in ordered water molecules and they were treated as water molecules during the refinement. The occupancy of the ligand in the secondary mode could be approximately estimated to be less than 25% of that in the principal mode by comparing the numbers of scattering electrons in Br and O (35:8).

For 2,4,6-tribromophenol (TBP), a modified model based on PBP was used because the structure was not available in the database. In the binding of the TBP, unlike PBP, the molecular twofold axis of the ligand was not coincident with the crystallographic twofold axis parallel to the *z* axis; the ligands occupied two symmetry-related sites each with 50% occupancy at each binding site.

Each model was subjected to cycles of positional refinement, simulated annealing and restrained isotropic atomic temperature-factor refinements. After each cycle of *B*-factor refinement, the models were examined on the graphics and refitted to the density. Water molecules were added to the atomic model using *WATERPICK* (in *X-PLOR*); they were placed at the positions of high positive ($>3.5\sigma$) peaks in the difference Fourier maps provided that they were (i) also present in the $2F_o - F_c$ electron-density map and (ii) in a suitable hydrogen-bonding environment. Water molecules whose temperature factors refined to values greater than 60 Å^2 were discarded from the model. Bulk-solvent corrections were applied and the lower resolution limit of the data included in the refinement was extended to 20 Å at a later stage of refinement. The first nine N-terminal residues and the last three or four C-terminal residues of TTR were not visible in any of the structures. The refined structures were analysed for geometric quality using *PROCHECK* (Laskowski *et al.*, 1993).[1] Atomic contacts between the protein, the ligands and

[1] Supplementary materials are available from the IUCr electronic archive (Reference: ad0111). Services for accessing these data are described at the back of the journal.

Table 1
Relative binding affinities of pentabromophenol and 2,4,6-tribromophenol for the T4 binding site on transthyretin.

Results shown are means ± standard deviation of at least triplicate measurements.

Structure	IC_{50} (n*M*)†	Relative potency‡	K_a (M^{-1}) (mean ± s.d.)§
Thyroxine	80.72 ± 1.21	1	$3.50 \pm 0.30 \times 10^7$
PBP	11.45 ± 1.78	7.14 ± 1.11	$2.56 \pm 0.40 \times 10^8$
TBP	67.25 ± 2.74	1.20 ± 0.05	$4.30 \pm 0.18 \times 10^7$

† IC_{50} values were determined from the competition curves and represent the concentration at 50% of total (^{125}I)-T_4 binding to TTR. ‡ Relative potencies are given as the ratio of $IC_{50}(T_4)/IC_{50}$ (competitor). § Binding-affinity constants are determined by the *LIGAND-PC* program (Munson & Rodbard, 1980).

the water molecules were calculated using *CONTACT* (Collaborative Computational Project, Number 4, 1994).

3. Results

3.1. Binding studies

Fig. 2 shows the competitive binding of PBP and TBP to transthyretin using ^{125}I-T_4 as the displaceable radioligand. Binding-affinity constants (K_a) were determined by non-linear curve fitting of T_4 displacement curves. The best-fit parameters are shown in Table 1. PBP is about seven times more potent than unlabelled T_4 in this assay system, while TBP has an affinity comparable to T_4.

3.2. X-ray crystallographic studies

A summary of the data-collection and refinement statistics for the native and the bromophenol-bound TTR structures is given in Table 2. The structures of the native TTR and TTR–bromophenol complex molecules at 100 K are very similar to that of native TTR at room temperature (Blake *et al.*, 1978; Hamilton *et al.*, 1992). The backbone structure of the protein remains unaltered by the introduction of the ligands into its binding channel, as has been the case for other ligand-bound TTR molecules (Blake & Oatley, 1977; Ciszak *et al.*, 1992; De la Paz *et al.*, 1992; Lans *et al.*, 1993; Peterson *et al.*, 1998; Wojtczak *et al.*, 1992, 1993, 1996).

Transthyretin is a tetrameric molecule formed by four monomers of an identical sequence of 127 residues and arranged in a 222 symmetry, three twofold axes intersecting at the centre of the molecule (Fig. 3*a*). One of these molecular twofold axes is coincident with the crystallographic twofold (*z*) axis, while the other two are coincident with the 2_1 (*x* and *y*) axes. Each monomer of TTR is a wedge-shaped β-barrel formed by two four-stranded sheets *hgad* and *febc*. Two such monomers (*A* and B) join edge-to-edge to form a dimer, stabilized by extensive antiparallel hydrogen bonding between the β-strands *h* and *f* at the edge of the monomers (Fig. 3*b*). The dimer *AB* thus formed is a pair of eight-stranded β-sheets with a pronounced concave shape because of the right-handed twist of the strands. A rotation of the dimer about the crystallographic twofold axis along *z* produces the tetramer

Table 2
Data-collection and refinement statistics.

Numbers in parentheses denote values in the highest resolution shell.

	Native	PBP†	TBP‡
Data collection			
Space group	$P2_12_12$	$P2_12_12$	$P2_12_12$
Unit-cell parameters (Å)			
a	42.7	43.0	42.8
b	85.4	85.4	84.9
c	64.2	64.3	64.4
Maximum resolution (Å)	1.75	1.8	1.8
Highest resolution shell (Å) of the data used	1.99–1.9	1.88–1.8	1.88–1.8
Total No. of observations	215400	119292	249678
Unique reflections	16505 (2102)	22174 (2762)	20818 (2543)
Completeness (%)	85.7 (88.7)	97.6 (99.4)	92.7 (92.8)
Mean $I/\sigma(I)$	22.1 (3.6)	21.2 (3.4)	29.4 (3.7)
Data with $I > 3\sigma(I)$§ (%)	85.9 (57.6)	83.4 (50.0)	85.2 (54.3)
Redundancy¶	3.2 (3.0)	2.6 (2.5)	3.7 (3.6)
R_{merge}†† (%)	3.9 (22.8)	5.8 (27.9)	4.8 (34.5)‡‡
Wilson *B* factor	28.3	21.7	24.5
Refinement			
Resolution range (Å)	20–1.9	20–1.8	20–1.8
No. of reflections	16447	22132	20764
R§§ (%)	19.3	19.3	21.4
R_{free}¶¶ (%)	25.2	23.5	26.2
No of water molecules	80	151	147
Average *B* (Å^2)			
Protein	33.3	23.4	19.4
Water	43.2	34.3	33.8
Ligand		35.3	45.8
R.m.s.d. bond lengths (Å)	0.009	0.007	0.008
R.m.s.d. bond angles (°)	1.5	1.4	1.4
R.m.s.d. dihedral angles (°)	27.5	26.8	26.4
R.m.s.d. impropers (°)	1.4	1.3	1.4
Ramachandran plot quality			
% in core allowed regions	88.6	89.1	89.6
% in additional allowed regions	11.4	10.9	10.4

† PBP, pentabromophenol. ‡ TBP, 2,4,6-tribromophenol. § No σ cutoff was applied. ¶ Average number of measurements for each reflection which contributed to the calculation of R_{merge}. †† $R_{merge} = \sum_{hkl}|\langle I_{hkl}\rangle - I_{hkl}|/\sum_{hkl}\langle I_{hkl}\rangle$, where $\langle I_{hkl}\rangle$ represents the average intensity of symmetry-equivalent reflections. ‡‡ Two data sets were collected from one TBP complex crystal; the R_{merge} for the highest resolution shell (1.88–1.8 Å) of the first data set was 24.5. A second data set, collected with a shorter exposure time per image to avoid overload of the strong reflections, was merged with the first one. Strictly speaking, the effective resolution of this merged data set of the TBP complex is 1.9 Å. However, the refinement was carried out including all data to 1.8 Å, because the significant part of the data was certainly reliable to 1.8 Å. §§ $R = \sum_{hkl}\left|(|F_o| - |F_c|)\right|/\sum(F_o)$, for a working set comprising of 95% of the data. ¶¶ $R_{free} = \sum_{hkl}\left|(|F_o| - |F_c|)\right|/\sum(F_o)$, for a test set comprising of 5% of the data selected randomly.

ABCD where the dimer–dimer interaction involves the edges of the concave sheets. This creates a 50 Å long central channel running through the entire length of the TTR molecule along the *z* axis, which has been identified as the hormone/ligand-binding site (Blake & Oatley, 1977).

There are two binding sites in this channel (*AC* between the monomers *A* and *C*, and *BD* between the monomers *B* and *D*), each of which has an intrinsic twofold symmetry as these are located on the *z* axis. When an asymmetric molecule such as a thyroid hormone binds to the protein, it binds in two different orientations symmetrically disposed about the twofold axis, each with a statistical probability of half occupancy (Fig. 4*a*). The sites *AC* and *BD* are structurally equivalent, being related to each other by a non-crystallographic symmetry axis. The extended binding site has a

hydrophilic region closest to the centre which comprises pairs of Ser112, Ser115, Ser117 and Thr119 from two monomers, followed by a hydrophobic region with pairs of Leu17, Ala108, Ala109, Leu110 and Val121. There are three pairs of symmetry-equivalent pockets in between the grooves of the β-sheets forming the binding cavity, in which the I atoms of T_4 bind. While the two I atoms (3,5) on the tyrosine ring of T_4 occupy the symmetrically related outer pockets at about 13 Å from the centre, the phenolic I atoms bind in two of the four inner pockets, which are not related by symmetry. In the native TTR structure the innermost 'distal' pockets at a distance of 6 Å from the centre are occupied by a pair of water molecules, which are displaced by one of the iodines (3′ or 5′) on the phenolic ring of T_4. The other phenolic I atom binds in the 'proximal' pockets, ∼9 Å from the centre.

3.2.1. TTR–pentabromophenol (PBP) complex. The difference Fourier and the electron-density map of the TTR–PBP complex showed the positions of PBP bound in the binding channel at two binding sites *AC* and *BD* between two sets of symmetry-related monomers of TTR (Fig. 4*b*), with no indication of binding anywhere else. The symmetrical molecules of PBP are bound, with their Br4 atoms at a distance $\simeq$ 7 Å from the centre of the TTR tetramer and the (Br4—OH) axis of the molecule coincident with the *z* axis. The peaks of Br atoms were the highest in the map (6σ) and unambiguously showed that PBP binds exclusively in the so-called 'reversed' mode as the OH group of the ligand does not point to the centre of the TTR tetramer but towards the mouth of the binding cavity.

The Br atoms Br4 are closest to the centre of TTR and interact with a pair of symmetry-related and well ordered water molecules at each binding site: *W*9/*V*9 at the *AC* end and *W*5/*V*5 at the *BD* end at a distance of 3.5–3.6 Å (Figs. 5*a* and 5*b*). (Water molecules are labelled *W* in one monomer and *V* in the symmetry-related monomer.) These water molecules are hydrogen bonded with pairs of Ser117 and Thr119 from neighbouring monomers and are also present in the native TTR structure, making similar interactions. The Br atoms adjacent to Br4 (Br3 and Br5) have extensive interactions with their nearest Thr119 (C^{β}, $C^{\gamma 2}$ and $O^{\gamma 1}$), as well as with Ala108 and Leu17. Most of the interactions here are hydrophobic in nature, except the one with Thr119 $O^{\gamma 1}$ (3.7 Å). The remaining Br atoms, Br2 and Br6, are adjacent to the hydroxyl group and are at a distance of about 12 Å from the centre of the TTR tetramer. These are in the hydrophobic environment of Val121, Leu17 and Lys15 from the two monomers on the two sides of the binding channel. However, they also interact with water molecules *W*217 (and *V*217) at a distance 3.5 Å at the *AC* end and with *W*229 (and *V*229) at a distance of 3.6 Å at the *BD* end of the molecule.

At the binding site between the monomers *B* and *D*, the ligand shows clear evidence of a second mode of binding

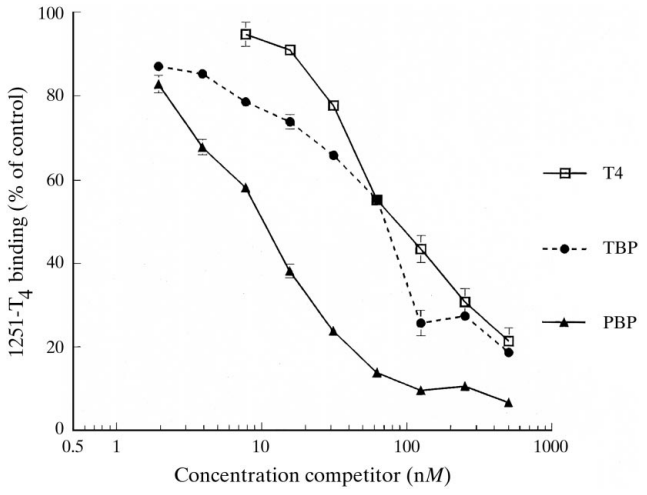

Figure 2
Competitive binding of pentabromophenol (PBP) and 2,4,6-tribromophenol (TBP) to transthyretin. Data are mean values of triplicate incubations. If no error bar is visible, it is smaller than the marker.

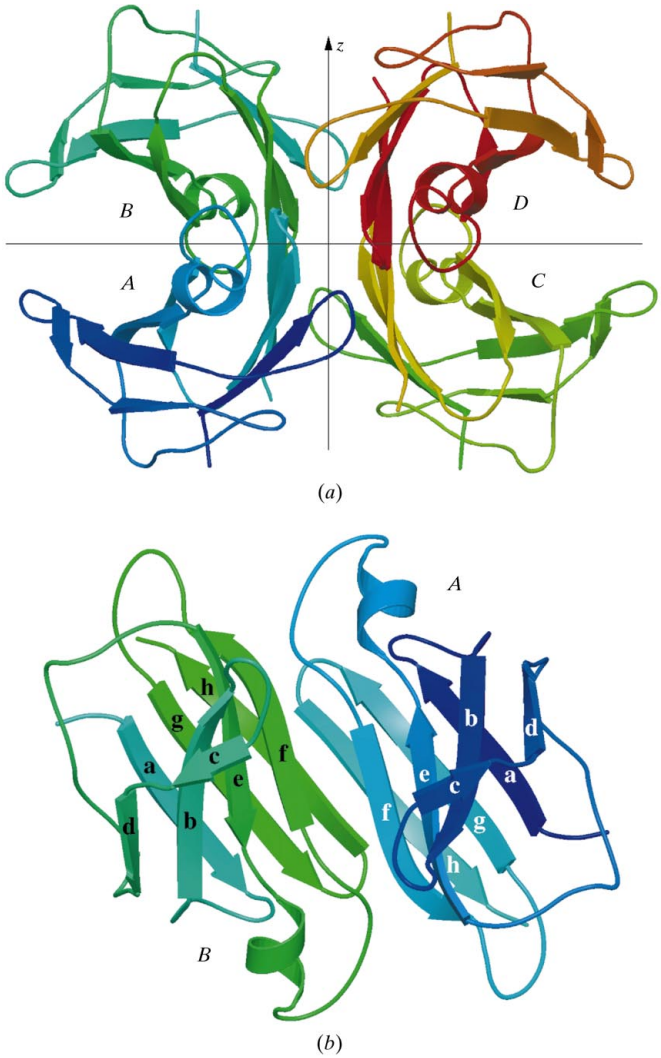

Figure 3
Ribbon diagram of transthyretin showing (*a*) the tetramer *ABCD*, with monomer *A*–*D* in colour ramping from blue to red. 50 Å long thyroxine-binding channel is shown along the *z* axis. (*b*) The monomers *A* and *B* joined side by side to form the dimer *AB*. The eight strands in each monomer are labelled *a*–*h*. The figures were created using the programs *BOBSCRIPT* (Esnouf, 1997) and rendered with *Raster3D* (Merritt & Murphy, 1994).

(termed PBP2) of lower occupancy in addition to the one just described (Fig. 4*b*). In this mode, the bound PBP molecule is still symmetrical about the channel axis with the axial atoms occupying identical positions, but the phenolic ring of the molecule is nearly at right angles to that in the principal mode. The interaction of the Br atoms are again mostly hydrophobic, with the residues Lys15, Leu17, Ala108, Ala109 and Leu110 (Fig. 5*b*), but there are also hydrophilic interactions with some main-chain and side-chain atoms. The electron density around the pair of Leu17 residues at this binding site is broad and indicates a disordered conformation of the residue to accommodate PBP Br atoms in two different modes. Some of the interatomic distances between Lys15 side-chain atoms and Br2 (and Br6) in this mode are much smaller (2.6–3.4 Å) than the acceptable van der Waals separation (3.3–3.5 Å). This probably suggests that in this mode the Lys15 residues assume a different conformation which is not detectable on the electron-density map as the occupancy is low. The interactions of the axial atoms of PBP remain unaffected as they have identical positions as in the principal mode.

The interaction with the OH group of the ligand at the mouth of the channel is different at the two ends of the molecule. At the *AC* end, the N^{ζ} of each Lys15 is locked in a triangular hydrogen-bond interaction with water molecules *W*217 (*V*217) and *W*64 (*V*64). It also interacts with the $O^{\varepsilon 1}$ of the corresponding Glu54 but not with the OH group of the ligand. At the *BD* end, Lys15 is strongly hydrogen bonded to the OH group of the ligand and the water molecules *W*/*V*229, but has no interaction with Glu54 residues. The contacts between PBP and TTR in the major binding mode PBP1 and the secondary mode PBP2 are listed in Tables 3(*a*) and 3(*b*).

The residues at the binding site of the TTR–PBP complex have very similar conformations to those of the native TTR at 100 K and at room temperature, except for Leu17 and Thr119. Both these residues undergo large rotations of about 120° to make space for Br3 and Br5 and to avoid steric hindrance.

3.2.2. TTR–2,4,6-tribromophenol (TBP) complex. The 2,4,6-tribromophenol molecule differs from pentabromophenol in the absence of Br atoms at the positions 3 and 5 (Fig. 1). This leads to a significant reduction in its binding

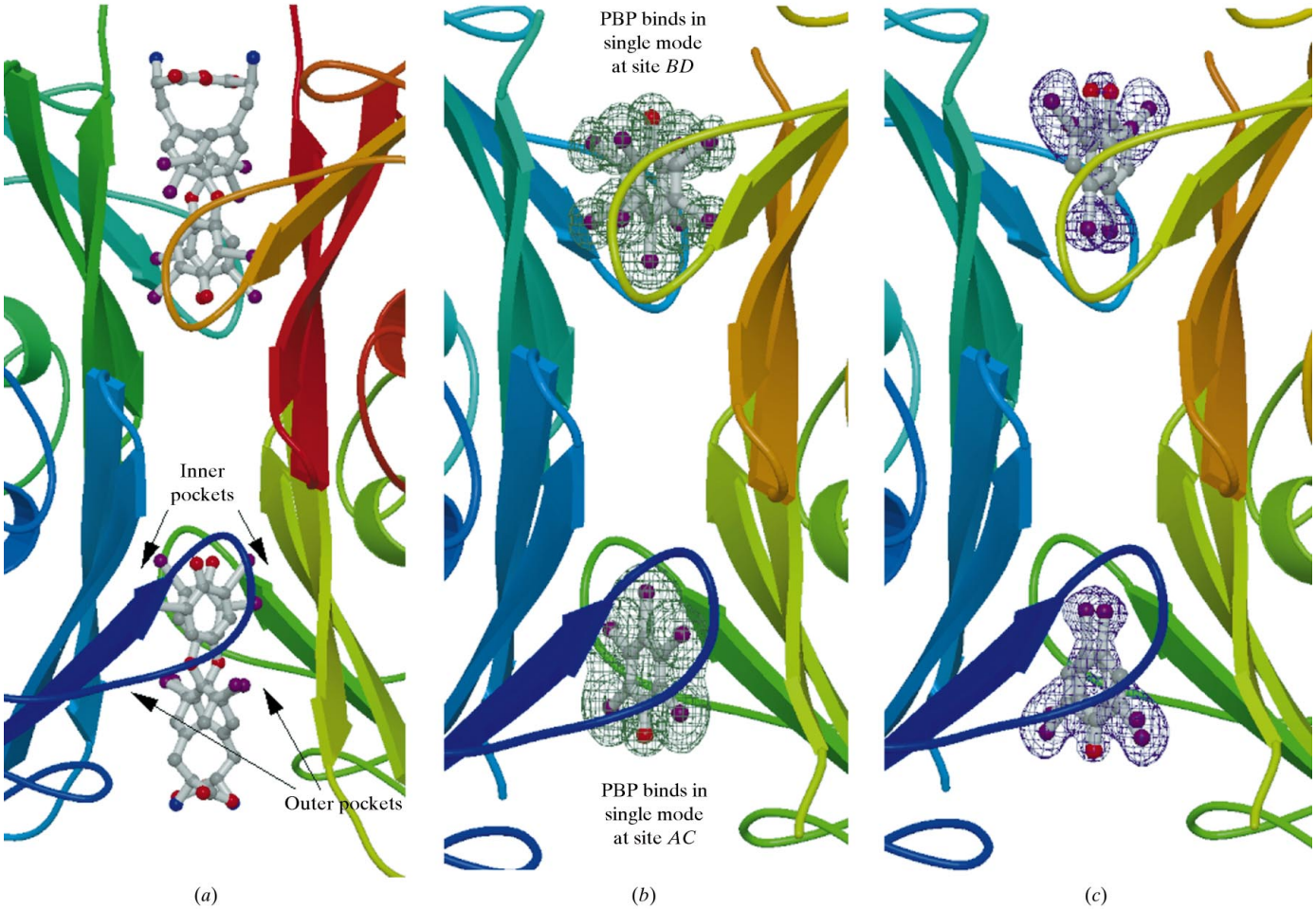

Figure 4
Diagrams showing the ligands in the TTR binding sites *AB* and *CD*; the halogens are in deep purple, O atoms in red, N atoms in blue and the C atoms are in grey. (*a*) In the TTR–T_4 complex, the asymmetric molecule of T_4 binds in two symmetry-related positions with half occupancy at each binding site. The I atoms on the phenolic rings bind in the inner pockets and those on the tyrosine ring bind in the outer pockets. (*b*) and (*c*), $2F_o - F_c$ maps around the ligands PBP and TBP, respectively, contoured at 1σ. The figures were created using the programs *BOBSCRIPT* (Esnouf, 1997) and rendered with *Raster3D* (Merritt & Murphy, 1994).

affinity with TTR as shown by the binding study. TBP binds exclusively in the 'reversed' mode at two sites in the TTR binding cavity (Fig. 4*c*), about 8 Å away from the centre of molecule and in an orientation similar to PBP. Unlike PBP, the molecular axis of TBP is slightly offset from the twofold *z* axis and at each binding site it occupies two symmetry-related positions with 50% occupancy. The binding of TBP molecules at the two sites at the *AC* and *BD* end of the molecule are similar but not identical. There is no secondary binding observed at either of these sites.

The interactions of TBP with the neighbouring residues are mostly similar to those in PBP, except for Leu17. The absence of Br atoms in positions 3 and 5 allows Leu17 residues to assume an orientation similar to that in the native TTR structure. The water molecules through which Br atoms Br2 and Br6 of PBP interact with the pair of Lys15 residues on the neighbouring monomers are absent in the TTR–TBP complex. Instead, the lysines interact directly with Br2 and Br6 (3.6 and 4.1 Å; Fig. 5*c*). The OH group of the molecule is almost on the *z* axis, and makes two symmetrical hydrogen bonds (3 Å) with the N^{ζ} atoms of the Lys15 residues at both end of the binding channel, in addition to a number of non-polar interactions with the same residue. The interaction of Br4 atoms with the conserved water molecules near the TTR centre (*W*46/*V*46 at the *AC* end and *W*58/*V*58 at the *BD* end) is similar, but is weak compared with that in PBP as the molecule does not bind as deep as PBP into the binding cavity. At the site *BD*, Br4 atoms have an additional interaction with an water molecule *W*336 located on the *z* axis, which is absent at the *AC* site as well as in the TTR–PBP complex. The separation between the two symmetry-related Br4 atoms at the site *BD* is wider (2.9 Å) than at the site *AC* (1.7 Å). The contact distances between TBP and surrounding residues of TTR are listed in Table 3(*c*).

4. Discussion

4.1. Unusual binding of PBP and TBP with TTR

Comparison of the TTR–PBP structure with that of TTR–T_4 (Blake & Oatley, 1977; Wojtczak *et al.*, 1996) shows that in the major binding mode PBP1 the ligand binds with its plane approximately at right angles to the phenolic planes of T_4 (Fig. 6*a*). While the Br atoms Br2 and Br6 occupy positions close to the outer I-atom positions I3 and I5 on the tyrosine ring of T_4, the other three Br atoms of the ligand are not in any conventional iodine pockets. For the secondary mode PBP2,

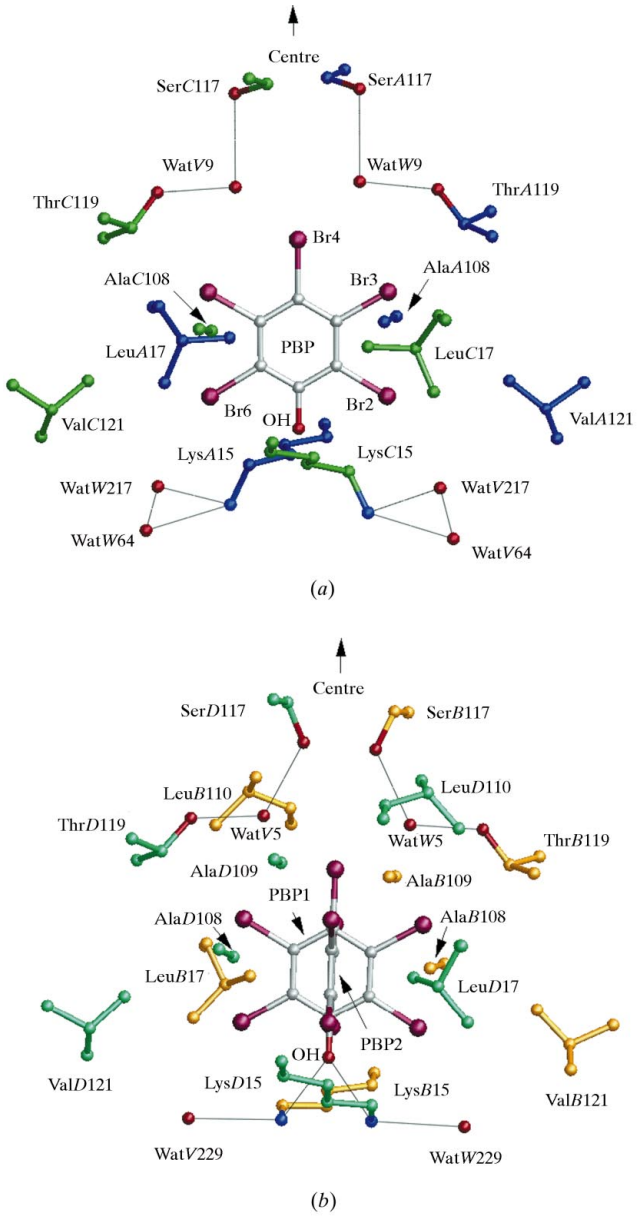

Figure 5
Interaction of the ligands with TTR residues and water molecules (*a*) at the binding site *AC* of the the TTR–PBP complex, where the ligand binds in single mode PBP1, (*b*) at the binding site *BD* of the TTR–PBP complex, where the ligand binds in double mode PBP1 and PBP2 with fractional occupancies, and (*c*) at the binding site *AC* of the TTR–TBP complex, where TBP binds in two symmetry-related positions with half occupancy. Hydrogen bonds are shown as thin lines. The figures were created using the program *XOBJECTS* (M. E. M. Noble, unpublished program).

Table 3
Interatomic distances.

Hydrogen bonds are in bold.

(*a*) Interatomic distances between TTR and PBP molecule in the primary mode.

	PBP primary binding site at			
	AC		*BD*	
Ligand atom	Protein atom	Distance (Å)	Protein atom	Distance (Å)
Br2	Wat*V*217 O	3.5	Wat*V*229 O	3.6
			Lys*D*15 N^{ζ}	3.6
			Leu*D*17 $C^{\delta1}$	3.1
Br3	Thr*A*119 C^{β}	3.5	Thr*B*119 C^{β}	3.6
			Leu*D*17 $C^{\delta1}$	3.2
Br4	Wat*W*9 O	3.5	Wat*W*5 O	3.6
	Wat*V*9 O	3.5	Wat*V*5 O	3.6
Br5	Thr*C*119 C^{β}	3.5	Thr*D*119 C^{β}	3.6
			Leu*B*17 $C^{\delta1}$	3.2
Br6	Wat*W*217 O	3.5	Wat*W*229 O	3.6
			Lys*B*15 N^{ζ}	3.6
			Leu*B*17 $C^{\delta1}$	3.1
O1			Lys*D*15 N^{ζ}	**2.9**
			Lys*B*15 N^{ζ}	**2.9**
C2			Leu*D*17 $C^{\delta1}$	3.3
C3			Leu*D*17 $C^{\delta1}$	3.3
C5			Leu*B*17 $C^{\delta1}$	3.3
C6			Leu*B*17 $C^{\delta1}$	3.3

(*b*) Interatomic distances between TTR and PBP molecule in the secondary binding mode, at the site *BD*†.

	PBP secondary binding site at *BD*	
Ligand atom	Protein atom	Distance (Å)
Br2	Lys*D*15 C^{β}	3.4
	Lys*D*15 C^{δ}	2.6
	Lys*D*15 C^{ε}	3.0
	Lys*D*15 C^{γ}	2.9
	Leu*D*17 $C^{\delta1}$	3.1
Br3	Ala*D*108 C^{β}	3.4
	Ala*D*109 N	3.6
	Ala*D*109 C	3.6
	Ala*D*109 O	3.5
	Leu*D*17 $C^{\delta1}$	3.2
Br5	Ala*B*109 O	3.6
	Leu*B*17 $C^{\delta1}$	3.2
	Ala*B*108 C^{β}	3.4
	Ala*B*109 N	3.6
	Ala*B*109 C	3.6
Br6	Lys*B*15 C^{ε}	3.0
	Leu*B*17 $C^{\delta1}$	3.1
	Lys*B*15 C^{δ}	2.6
	Lys*B*15 C^{β}	3.4
	Lys*B*15 C^{γ}	2.9
C2	Leu*D*17 $C^{\delta1}$	3.3
C3	Leu*D*17 $C^{\delta1}$	3.3
C5	Leu*B*17 $C^{\delta1}$	3.3
C6	Leu*B*17 $C^{\delta1}$	3.3

Table 3 (continued)

(*c*) Interatomic distances between TBP and TTR at the two binding sites.

	TBP binding at the site			
	AC		*BD*	
Ligand atom	Protein atom	Distances (Å)	Protein atom	Distances (Å)
Br2	Leu*C*17 $C^{\delta1}$	3.6		
			Lys*B*15 N^{ζ}	3.4
Br4			Leu*B*17 $C^{\delta1}$	3.4
			Wat*W*336 OH	3.3
Br6	Lys*A*15 N^{ζ}	3.6	Lys*D*15 N^{ζ}	3.6
O1	Lys*A*15 N^{ζ}	**3.0**	Lys*B*15 N^{ζ}	**2.8**
	Lys*C*15 N^{ζ}	**3.1**	Lys*D*15 N^{ζ}	**3.0**
C3			Leu*B*17 $C^{\delta1}$	2.9
C5	Leu*A*17 $C^{\delta1}$	3.2		

† The distances between the protein and the ligand atoms Br4 and O1 are identical to those in primary mode.

however, the ligand is in similar orientation as the phenolic ring in T_4: Br3 and Br5 occupy the inner proximal pockets (I3′ and I5′) of T_4 (Fig. 6*b*). In both PBP1 and PBP2, Br4 has a position close to and in the middle of the two positions where the OH groups of T_4 bind. Thus, in each mode, only two of the five Br atoms of the ligand can occupy the iodine pockets of T_4. The crucial difference between the two molecules that forces PBP to assume such an unusual binding position lies in the fact that the Br atoms in PBP are coplanar, while the I atoms in T_4 attached to the phenolic ring (3′,5′) and the tyrosine ring (3,5), have a pseudo-tetrahedral arrangement which matches the positions of the halogen pockets in the TTR-binding cavity. Any two of the PBP Br atoms can thus occupy the positions of T_4 I atoms either on the phenolic ring or those on the tyrosine ring. As the twofold symmetry of the site coincides with that of the PBP molecule, the ligand rotates about its molecular axis and chooses one of the two options. The other three Br atoms are restricted to positions in the same plane, even though these are not the conventional halogen-binding pockets.

Interestingly, PBP in its principal binding mode PBP1 prefers the position where Br2 and Br6 occupy the iodine pockets of the T_4 tyrosine ring (the so-called outer pockets) and *not* the positions where its Br3 and Br5 atoms fill in the inner proximal pockets, which remains a possible binding option as is shown in the low-occupancy secondary mode. Binding of halogens at these outer pockets depends on the interactions between the bromines and the neighbouring residues which play an important deciding role in the way the ligands bind. In the principal mode of PBP1, each of the non-axial atoms in the ligand makes a number of contacts, mainly hydrophobic, with *both* the monomers. This would increase the stability of the dimers *AC* and *BD*. In the secondary binding mode, observed only at one site, such interactions are limited to just one monomer, *i.e.* one half of the molecule is entirely in the environment of and interacting with the monomer *B*, while the other half is interacting with *D*. The atoms on the axis of the ligand occupy identical positions in both modes and interact with both monomers.

The binding pattern in the TTR–TBP complex reinforces the observation that the outer T_4 pockets where Br2 and Br6 bind provide a more suitable environment for halogen binding. The positions of these Br atoms in two symmetry-related orientations of the ligand are not coincident as is the case in TTR–PBP but are separated by a small distance as are

the I atoms in the TTR–T_4 complex. The separation is 0.5 Å (0.8 Å for TTR–T_4) at the *AC* end compared with 1.4 Å (1.6 Å for T_4) at the *BD* end, *i.e.* the pockets are extended over a smaller area at the *AC* end. The exact position of the pockets has also been found to be quite flexible in other complex structures and is determined by the interaction of the halogens with the neighbouring residues and the steric hindrance the ligand molecule experiences at the narrow central part of the binding channel.

The interactions of Br4, the Br atoms which are in a polar environment at the centre of the TTR molecule, are quite exceptional. In other TTR complex structures, it is usually the OH group of the phenolic ring in the forward mode (or the amino-acid side chain in case of a reversed mode of entry) which interacts with the polar residues and the bound water molecules at the centre. A search through the *Isostar* (Lommerse *et al.*, 1996) database shows that polar reactions of aromatic Br atoms are relatively uncommon, although it has been observed (Bruno *et al.*, 1997) that carbon-bonded halogens (with the exception of fluorine) can form contacts with electronegative atoms such as oxygen, nitrogen and sulfur and that the contact distance can be smaller than the sum of the van der Waals radii in the direction of the bond connecting the C atom and the halogen. This has been explained in terms of an anisotropic electron distribution of the halogen atoms which results in a decreased repulsive wall and an increase in the electrostatic attraction in the direction of the carbon–halogen bonds. In these two TTR complexes, most of the contact distances are within the range 3.5–3.8 Å, which exceeds the sum of van der Waals radii of oxygen and bromine (3.35 Å). The 3.3 Å contact distance between two symmetrical Br4 atoms and the axial water molecule *W*336 at the *BD* end in the TBP complex is the only interaction which is shorter than the sum of van der Waals radii and it makes an angle of 138° with the C4—Br4 bond.

The water molecules near the centre of the binding channel of the bromophenol complexes form part of an extensive network of hydrogen bonds with residues Ser112, Ser115, Ser117 and Thr119, which also exists in the native TTR tetramer. The halogens, through their interactions with these water molecules, contribute to the links that hold the subunits together. This probably explains the considerably higher affinity of PBP in comparison to TBP. A similar increase in the binding affinity has been observed for TTR–chlorophenol complexes from monochlorophenol to pentachlorophenol, in proportion to the number of chlorine substituents (Van den Berg, 1990).

A significant difference between the dimers has been observed in all the three structures, namely in the loop connecting the strands *f* and *g*, residues 97–104. This loop is ordered and has good density for the monomers *A* and *C*, whereas in *B* and *D* this is disordered. The *g* strand lies in between the strands *a* and *h*, *i.e.* between the N- and C-termini. The first nine and the last 3/4 residues of TTR have not been observed in any X-ray structure [with one exception of the 1.7 Å structure of wild type and the amyloidogenic variant Val30-Met30 TTR (Hamilton *et al.*, 1992), where the N- and C-termini were modelled and refined to fit the disconnected densities observed in the vicinity of the termini], presumably because of the flexible nature of the chain in these two regions. There has been speculation (Wojtczak *et al.*, 1993) about the role that these mobile termini play in ligand binding because of their proximity to the entrance of the binding channel.

The dissimilar binding of the ligand molecules and the difference in the various interactions at the two binding sites observed in these two complex structures provides the first X-ray evidence that the *AC* and *BD* dimers are not identical in their interactions. In all TTR–ligand complex structures prior to this current study, the binding of ligands at the two sites were found to be similar. Chemical evidence, however, showed that for T_4 and several other hormone analogues, these binding sites have different affinity. For T_4, only one molecule binds with high affinity $\simeq 10^8\ M^{-1}$ (Raz & Goodman, 1969; Nilsson & Peterson, 1971; Pages *et al.*, 1973), while the second site has an affinity 100-fold less than the first site (Cheng *et al.*, 1977). The exact reason for such disparity is yet to be understood.

4.2. Reversed binding and comparisons with other ligand structures

The other interesting feature observed in these two complex structures, that the ligands bind exclusively in a reversed mode with their hydroxyl groups pointing towards the mouth of the binding cavity, is a rare occurence. The only other example of such exclusive reversed binding has been observed in the

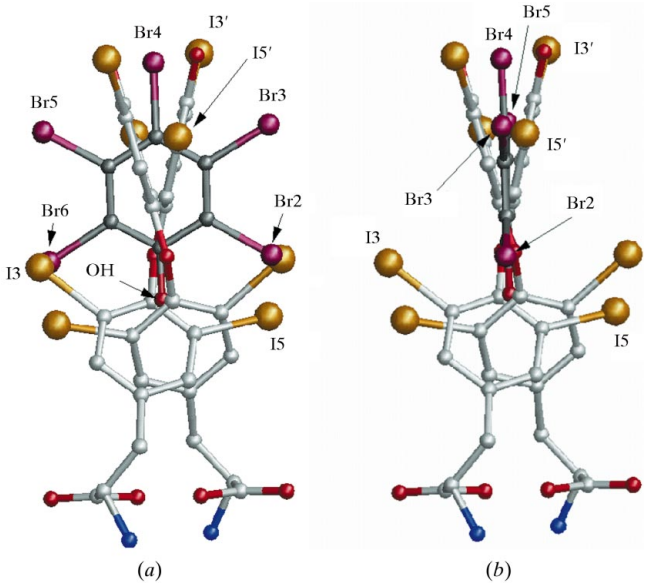

Figure 6
Superposed view of thyroxine on the ligand PBP at the TTR–PBP binding site. (*a*) In its principal binding mode PBP1, the Br atoms Br2 and Br6 occupy the outer pockets of thyroxine while (*b*) in the secondary binding mode PBP2, Br3 and Br5 are in the inner pockets of the hormone. I atoms are shown in gold and Br atoms are in rust red. The figures were created using the program *XOBJECTS* (M. E. M. Noble, unpublished program).

TTR–flufenamic acid complex (Peterson *et al.*, 1998), where the CF_3 substituents occupy the innermost pockets and the carboxylate group on the outer phenyl ring is located near the entrance of the binding cavity, interacting with Lys15s.

The possibility of partial reversed binding in addition to the more common 'forward binding' has been discussed (De la Paz *et al.*, 1992) with reference to the TTR complexes with 3′,5′-diiodo-L-thyronine (3′,5′-T_2), 3,3′-diiodo-L-thyronine (3,3′-T_2) and 3,3′,5′-triiodo-L-thyronine (reverse T_3/RT_3). In the light of these observations, the results of TTR–T_4 and TTR–T_3 could also be reinterpreted in terms of a mixture of a forward and reversed binding. It was concluded that 3′,5′–T_2 and RT_3 bind in a combination of reversed and forward mode in an estimated ratio of 60:40. The ligand 3,3′-T_2 binds in the reverse mode as well as two different types of forward mode, one translated further into the binding cavity with respect to the other and occupying only the inner pockets. These complexes were prepared by soaking the native crystals with concentrated solutions of the appropriate ligand for a long time. In another structural study on 3,3′-T_2 (Wojtczak *et al.*, 1992), where the complex crystals were obtained by co-crystallization, the ligand binds in the translated forward mode only, about 3 Å deeper into the channel. It is thus seen that for the same ligand, the binding can be different depending on how the complex was prepared. Two sets of forward binding were also observed in the TTR–3′,5′-dibromo-2′,4,4′,6-tetrahydroxyaurone complex (Ciszak *et al.*, 1992), where the phenolic Br atoms of the ligand bind in the outer pockets exactly where the Br2 and Br6 of PBP bind, as well as in the innermost pockets occupied by the ordered water molecules in PBP. The translated forward binding deeper into the binding channel was possible for these two compounds as there is only one iodine substituent on the phenolic ring for the first compound; for the second compound, the distance between two Br atoms on the phenolic ring is shorter than that between two I atoms.

Thus, there are a number of ways in which TTR can accommodate different ligands. The overall preferences of binding are, however, for the outer pockets, with the inner proximal pockets having the least probability of occupancy. For the reverse binding of the thyroid hormones, when the amino-acid side chain of the hormone is at the TTR centre, the outer pockets are a distance of 14 Å from the centre. However, for ligands in forward binding, with no halogens at the 3′,5′ position, the outer pockets can be as close as 12 Å from the centre. For PBP, this distance is also 12 Å, in spite of being in the reverse mode, as in this case there is no amino-acid side chain to be accommodated at the centre. Compared with this, TBP has its outer pockets at ∼13 Å from the centre. Most certainly the missing interactions of the Br3 and Br5 cause the TBP molecule to bind slightly away from the centre.

In the translated forward binding mode, the OH groups of the compounds are within the hydrogen-bonding distance from the O^{γ} atoms of the four Ser117 residues at the centre of the tetramer. Similar hydrogen bonds were found in the structure of TTR–4,4′-$(OH)_2$-3,3′,5,5′-tetrachlorobiphenyl complex (Lans *et al.*, 1993), where it has been argued that this hydrogen-bond formation may be an important requirement for strong binding of OHSs to TTR, as the parent compound without this hydroxyl group did not bind TTR (Brouwer *et al.*, 1990). The current study on the bromophenol complexes, however, has shown that strong binding can take place even in the absence of such a hydrogen-bond interaction of the OH group of the ligand with the Ser117 residues. This agrees with the observation that TTR binds with non-hydroxylated compounds (Chauhan *et al.*, 1998; Rickenbacher *et al.*, 1986), though the binding is weak and may imply that a much larger number of OHSs present in the environment have the potential to compete with thyroxine and hence adversely affect the thyroid hormone system in animal and human.

In summary, some interesting new features have been observed in the binding of PBP and TBP to human transthyretin. The outer pockets in the TTR-binding channel seem to be the most favoured sites for these single-ring organohalogen compounds, as observed in some other complexes. The binding in the outer pockets gives the ligands greater freedom to make stable binding interaction, while the inner sites may be more restrictive. The symmetric disposition of the bromines about the O—Br4 axis in PBP and TBP molecules has allowed the symmetry-related bromines to be accommodated in the TTR channel in a way that these atoms can conform to the inherent twofold symmetry of the binding channel and participate in energetically equivalent interactions. Forward binding has not been observed at all for these two bromophenol complexes, because the reversed binding provided the hydroxyl group with a more polar environment.

We thank Drs C. C. F. Blake, M. J. Adams and S. Gover for valuable discussions at various stages of the work and manuscript preparation, Dr E. Garman for training MG in cryocrystallography, Drs R. K. Bryan and Y. Huang for help in computing and Mr S. Lee for assistance in photography. All the above are members or ex-members of the Laboratory of Molecular Biophysics, Oxford, England. We thank Dr K. J. Van den Berg, TNO Nutrition, Zeist, the Netherlands for the *LIGAND-PC* program and Ms S. Rahm, Environmental Chemistry, Stockholm University, Sweden for purifying the bromophenols used in crystallography. This work has been supported by EU contract no ENV4-CT96-0170.

References

Allen, F. H. & Kennard, O. (1993). *Chem. Des. Autom. News*, **1**, 31–37.

Blake, C. C. F., Geisow, M. J., Oatley, S. J., Rerat, C. & Rerat, B. (1978). *J. Mol. Biol.* **88**, 339–356.

Blake, C. C. F. & Oatley, S. J. (1977). *Nature (London)*, **268**, 115–120.

Brouwer, A., Klasson-Wehler, E., Bokdam, M., Morse, D. C. & Traag, W. A. (1990). *Chemosphere*, **20**, 1257–1262.

Brouwer, A., Morse, D. C., Lans, M. C., Sachuur, A. G., Murk, A. J., Klasson-Wehler, E., Bergman, A. & Visser, T. J. (1998). *Toxicol. Ind. Health*, **14**, 59–84.

Brünger, A. T. (1992). *X-PLOR. Version 3.1. A System for X-ray Crystallography and NMR.* New Haven, Connecticut and London: Yale University Press.

Bruno, I. J., Cole, J. C., Lommerse, J. P. M., Rowland, R. S., Taylor, R. & Verdonk, M. L. (1997). *J. Comput. Aid. Mol. Des.* **11**, 525–537.
Chauhan, K. R., Kodavanti, P. R. S. & Mckinney, J. D. (1998). *Organohalogen Comp.* **37**, 101–104.
Cheng, S. Y., Pages, R. A., Saroff, H. A., Edelhoch, H. & Robbins, J. (1977). *Biochemistry*, **16**, 3707–3713.
Ciszak, E., Cody, V. & Luft, J. R. (1992). *Proc. Natl Acad. Sci. USA*, **89**, 6644–6648.
Collaborative Computational Project, Number 4 (1994). *Acta Cryst.* D**50**, 760–763.
De la Paz, P., Burridge, J. M., Oatley, S. J. & Blake, C. C. F. (1992). *The Design of Drugs to Macromolecular Targets.*, edited by C. R. Beddell, pp. 119–171. New York, USA: John Wiley & Sons Ltd.
Esnouf, R. M. (1997). *J. Mol. Graph.* **15**, 132–134.
Garman, E. F. & Schneider, T. R. (1997). *J. Appl. Cryst.* **30**, 211–237.
Hamilton, J. A., Steinrauf, L. K., Braden, B. C., Liepnieks, J., Benson, M. D., Holmgren, G., Sandgren, O. & Steen, L. (1992). *J. Biol. Chem.* **268,** 2416–2424.
Jones, T. A. & Kjeldgaard, M. (1997). *Methods Enzymol.* **277**, 173–208.
Lans, M. C., Klasson-Wehler, E., Willemsen, M., Meussen, E., Safe, S. & Brouwer, A. (1993). *Chem. Biol. Interact.* **88**, 7–21.
Lans, M. C., Spiertz, C., Brouwer, A. & Koeman, J. H. (1994). *Eur. J. Pharmacol.* **270**, 129–136.
Laskowski, R. A., MacArthur, M. W., Moss, D. S. & Thornton, J. M. (1993). *J. Appl. Cryst.* **26**, 283–291.
Lommerse, J. P. M., Stone, A. J., Taylor, R. & Allen, F. H. (1996). *J. Am. Chem. Soc.* **118**, 3108–3116.
Meerts, I. A. T. M., van Zanden, J. J., Luijks, E. A. C., van Leeuwen-Bol, I., Marsh, G., Jakobsson, E., Bergman, A. & Brouwer, A. (2000). *Toxicol. Sci.* **56**, 95–104.
Merritt, E. A. & Murphy, M. E. P. (1994). *Acta Cryst.* D**50**, 869–873.
Munson, P. J. & Rodbard, D. (1980). *Anal. Biochem.* **107**, 220–239.
Nilsson, S. F. & Peterson, P. A. (1971). *J. Biol. Chem.* **246**, 6098–6105. (1971).
Otwinowski, Z. & Minor, W. (1997). *Methods Enzymol.* **276**, 307–326.
Pages, R. A., Robbins, J. & Edelhoch, H. L. (1973). *Biochemistry*, **12**, 2773–2779.
Peterson, S. A., Klabunde, T., Lashual, H. A., Purkey, H., Sacchettini, J. C. & Kelly, J. W. (1998). *Proc. Natl Acad. Sci. USA*, **95**, 12956–12960.
Pluim, H. J., De Vijlder, J. J. M., Olie, K. & Koppe, J. G. (1993). *Environm. Health Perspect.* **101**, 504–508.
Raz, A. & Goodman, D. S. (1969). *J. Biol. Chem.* **244**, 3230–3237.
Rickenbacher, U., McKinney, J. D., Oatley, S. J. & Blake, C. C. F. (1986). *J. Med. Chem.* **29**, 641–648.
Robbins, J. (1991). *The Thyroid: a Fundamental and Clinical Text*, edited by L. E. U. Braveman, pp. 111–125. Philadelphia, USA: J. B. Lippincott and Co.
Safe, S. H. (1994). *Crit. Rev. Toxicol.* **24**, 87–149.
Somack, R., Nordeen, S. K. & Eberhardt, N. L. (1982). *Biochemistry*, **21**, 5651–5660.
Van den Berg, K. J. (1990). *Chem. Biol. Interact.* **76**, 63–75.
Van den Berg, K. J., Zurcher, C. & Brouwer, A. (1988). *Toxicol. Lett.* **41**, 77–86.
Van Raaij, J. A. G. M., Van den Berg, K. J. & Notten, W. R. F. (1991). *Toxicol. Lett.* **59**, 101–107.
Wojtczak, A., Cody, V., Luft, J. R. & Pangborn, W. (1996). *Acta Cryst.* D**52**, 758–765.
Wojtczak, A., Luft, J. R. & Cody, V. (1992). *J. Biol. Chem.* **267**, 353–357.
Wojtczak, A., Luft, J. R. & Cody, V. (1993). *J. Biol. Chem.* **268**, 6202–6206.